applied optics

Measurements of seeing-induced crosstalk in tip–tilt corrected solar polarimetry

Harsh Mathur,[1,*] K. Nagaraju,[1] Hemanth Pruthvi,[2] and K. Sagaynathan[1]

[1]Indian Institute of Astrophysics, II Block, Koramangala, Bengaluru 560 034, India
[2]Thüringer Landessternwarte Tautenburg, Sternwarte 5, 07778 Tautenburg, Germany
*harsh.mathur@iiap.res.in

Received 17 January 2024; revised 15 April 2024; accepted 28 April 2024; posted 29 April 2024; published 16 May 2024

We present measurements of seeing-induced crosstalk using spectropolarimetric observations of sunspots recorded simultaneously in the H α and Ca II 8662 Å lines with the Kodaikanal Tower Tunnel (KTT) telescope. The Kodaikanal Tower Tunnel telescope is integrated and installed with an image stabilization system consisting of a tip–tilt and an autoguider system. Additionally, the spectropolarimeter at KTT is upgraded to allow for the simultaneous recording of spectropolarimetric observations in three spectral lines. The tip–tilt system is shown to have a cutoff frequency of 80 Hz, effectively reducing the seeing induced crosstalk in the measured Stokes parameters by at least a factor of 2.

https://doi.org/10.1364/AO.519245

1. INTRODUCTION

Accurate measurements of the solar magnetic field are crucial for understanding solar activity and its effects on our solar system. To infer solar vector magnetic fields through their imprints on the emergent spectra through the Zeeman and Hanle effects, accurate measurements of the polarization of light are required. Ground-based spectropolarimetric observations offer distinct advantages over measurements from space-based observatories like the Spectropolarimeter at Hinode (Hinode-SP) and Helioseismic and Magnetic Imager/Solar Dynamics Observatory (HMI/SDO). For high-resolution studies of specific solar regions, such as the quiet Sun, active regions, and plages, large aperture telescopes are essential. These telescopes excel in capturing ample light and delivering superior spatial resolution, enabling the detailed study of intricate solar features. Nonetheless, ground-based measurements face challenges, particularly atmospheric turbulence that leads to random image aberrations that degrade spatial resolution and introduce spurious polarization [1–3]. Atmospheric seeing causes random image distortions on very short time scales (on the order of a few milliseconds), which randomly spreads the signal rapidly from one pixel to the other. The spurious polarization, also known as seeing-induced crosstalk, is a result of the nonsimultaneous nature of the polarization measurement process. As the detectors are not directly sensitive to polarization but only to intensity, the polarization signal is encoded (also known as polarization modulation) in terms of the intensity variation, and the input signal is retrieved by decoding (demodulation) this intensity variation [4]. A minimum of four intensity measurements are required to retrieve the input beam's complete polarization information (all four Stokes parameters I, Q, U, and V). Unless these intensity measurements are completed within a few milliseconds, the measurement process results in a crosstalk among the Stokes parameters. To address these issues, technologies like tip–tilt and adaptive optics (AO) are employed to enhance the image stability and minimize the impact of atmospheric distortions, thus improving the precision of ground-based solar magnetic field measurements [5].

Lites [1] developed a Fourier transformation-based method to analyze crosstalk arising from atmospheric seeing, initially concentrating on tip–tilt effects linked to image motion. His work revealed that increasing the modulation frequency effectively reduces crosstalk. Building upon Lites' work, Judge *et al*. [2] further investigated residual image motion following tip–tilt correction through AO. They explored both rotating-wave plate and discrete modulation approaches using liquid crystal variable retarders, concluding that improved correction of higher-order image aberrations results in reduced seeing-induced crosstalk. Consequently, combining a polarimeter with AO is anticipated to significantly reduce crosstalk in polarization measurements induced by atmospheric seeing. Nagaraju and Feller [3] and Nagaraju *et al*. [6] in their simulations assessed the impact of higher-order aberrations and observed that the crosstalk among Stokes parameters remains practically unaffected by the extent of image aberration correction achieved by an AO system at high modulation frequencies. However, higher-order AO corrections enhance the signal-to-noise ratio by reducing the blurring caused by atmospheric seeing.

In this study, we assess the impact of the tip–tilt system on the reduction of the seeing-induced crosstalk present among Stokes parameters in both the H α and Ca II 8662 Å spectra by comparing measurements taken with and without the tip–tilt system.

The measurements are obtained with a spectropolarimeter [7] at KTT [8], which has been upgraded to enable simultaneous recording of spectropolarimetric observations in three spectral lines. We also discuss the tip–tilt system's performance and limitations.

2. OBSERVATION SETUP

The data were acquired using the Kodaikanal Tower Tunnel Telescope [8], which has a three-mirror Coelostat placed in the tower as a light feeding system. The primary mirror (M1) is responsible for tracking the Sun, while the secondary mirror (M2) redirects the sunlight downward. The tertiary mirror (M3) makes the beam horizontal and is followed by an achromatic doublet (effective aperture 38 cm, f/96), which focuses the Sun's image at a distance of 36 m with an image scale of $5\overset{''}{.}5\ \mathrm{mm}^{-1}$. M2 is further enhanced with a stepper motor, allowing adjustments in both North–South and East–West directions. This mechanism enables the movement of M2, consequently shifting the Sun's image on the image plane. This arrangement facilitated the development of an autoguider system for the telescope; more details are given in Mathur *et al*. [9]. A tip–tilt system, a concept demonstrated by Pruthvi [10], has been incorporated into the autoguider system, called the image stabilization system. In this updated configuration, the C-Blue One camera from First Light Imaging is utilized, substituting the Andor Neo sCMOS camera, to serve as the tip–tilt camera.

Using the polarimeter developed by Pruthvi *et al*. [7], spectropolarimetric observations in the Ca II 8662 Å and H α lines were recorded simultaneously, with and without the tip–tilt system. Figure 1 shows a schematic of the tip–tilt and polarimeter setup at KTT. The light from the telescope (f/96) is directed to the modulation unit via a tip–tilt mirror affixed to a piezo actuator PSH10/2 from Piezosystem Jena. Within the modulation unit, there are a quarter-wave plate and a half-wave plate at 630 nm. Subsequently, the light passes through a dichroic beam displacer, which redirects the blue beam (with a wavelength less than 600 nm) to the tip–tilt camera, a C-Blue One from First Light Imaging. The piezo actuator and tip–tilt camera forms the tip–tilt system. Meanwhile, the science beam is transmitted to another fold mirror, which also functions as the scanning mirror. This mirror reflects the science beam toward a polarizing beam displacer, splitting the light into two orthogonally polarized components. Both polarized components then traverse through an achromatic quarter-wave plate and continue to the slit of the Littrow mount grating-based spectrograph. The dispersed light from the grating falls onto the detector(s). The typical exposure time per slit position per modulation state per integration frame is 500 ms. A four-stage modulation scheme was used with a total of five integration frames recorded per modulation state. Consequently, one set of measurements were recorded in 10 s (modulation frequency = 0.1 Hz).

To record the H α and Ca II 8662 Å spectra, we installed two new cameras: the Kinetix from Teledyne (NUV and visible) and the ORCA-Quest from Hamamatsu (visible and NIR) at the spectrograph focal plane. However, accommodating three cameras at the spectrograph focal plane was not directly supported at KTT. To address this limitation, we have designed, in-house

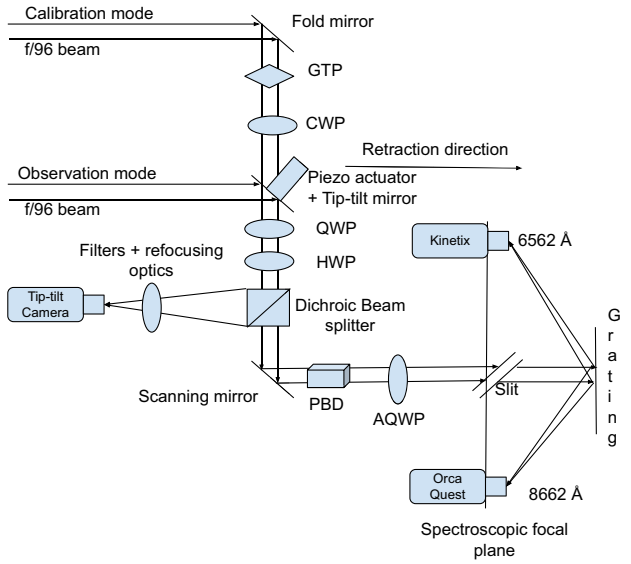

Fig. 1. Optical layout of the tip–tilt system and the polarimeter setup at KTT. In observation mode, light from the telescope is fed to the modulation unit by a tip–tilt mirror that is glued to the piezo actuator. It passes through quarter-wave plate (QWP), half-wave plate (HWP), and dichroic beam splitter (DBS) that transmits light of wavelength above 600 nm. It is then reflected by another fold mirror (scanning mirror) and passes through a polarizing beam displacer (PBD) that splits the beam in to two with orthogonal states of polarization, followed by an achromatic quarter wave plate (AQWP). In the calibration mode, light from the telescope is fed to the calibration unit by yet another folding mirror. It then passes through a Glan-Thompson polarizer (GTP) and a quarter-wave plate (CWP), producing light with a known state of polarization. In this mode, the tip–tilt mirror is retracted and the light is allowed to pass through the modulation unit and so on. The blue beam, with a wavelength less than 600 nm, passes through the DBS and proceeds to the tip–tilt camera, a C-Blue One from First Light Imaging.

manufactured, and installed a camera mount specifically tailored for the KTT spectrograph. This new mount can support up to three cameras, and it accommodates both C- and F-mount cameras. Moreover, the positions of the cameras are adjustable, allowing observers to record spectra simultaneously in three spectral regions of interest within the limitations of the space availability at the spectral focal plane.

To synchronize the capture and readout of the three cameras, the polarimeter software was updated accordingly. These adaptations enabled us to perform simultaneous spectropolarimetric observations in the desired spectral lines. In our upcoming paper, we will present our work focused on inferring the stratification of the magnetic field inferred using the spectropolarimetric observations recorded in the Ca II 8662 Å line. The magnetic field inferred will be compared from the application of the weak field approximation to the Stokes profiles in the H α line.

3. TIP–TILT SYSTEM PERFORMANCE AND LIMITATIONS

The top row of Fig. 2 presents a comparison of the power spectrum of image motion with and without the tip–tilt system

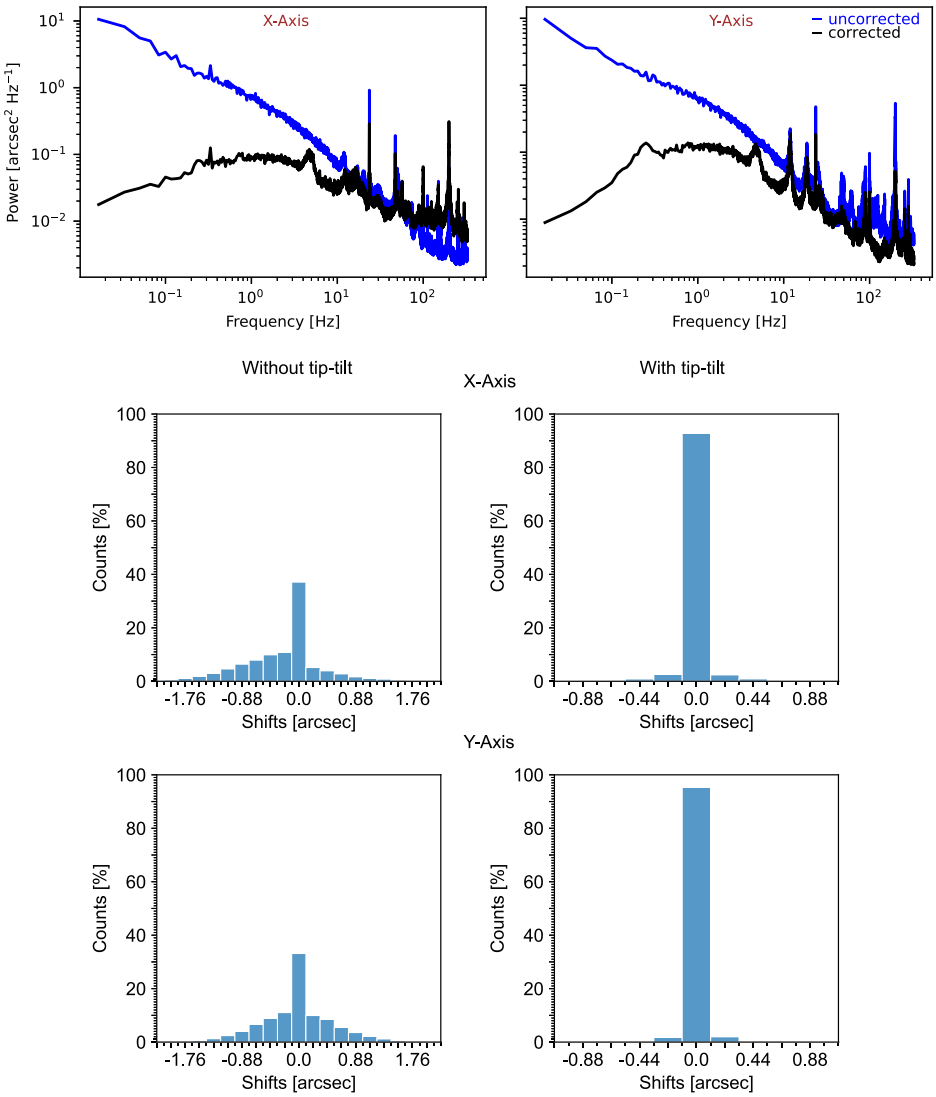

Fig. 2. Performance of the image stabilization system. The panels in the top row compare the power spectra of the image motion with and without tip–tilt correction (duration 1 h). The panels in the bottom two rows show the histogram of the image motion in the pixel scale before and while tip–tilt system is in use. The system reaches a point of diminishing returns in reducing image motion above approximately 80 Hz.

recorded by the tip–tilt camera using a broadband filter with a center wavelength at 550 nm and a FWHM of 80 nm. The histogram of the image motion is presented in the bottom two rows. The spectrum without tip–tilt is derived from the image motion data recorded when only the image autoguider [9] system was operational. In contrast, the spectrum with tip–tilt is calculated from data recorded when both the tip–tilt and autoguider systems were operational. Both spectra were computed from data recorded for a duration of 1 h.

Before implementing the tip–tilt system, only around 40% of the time did the image motion remain within $\pm 0\overset{''}{.}11$. However, this percentage significantly improves to about 95% when the tip–tilt system is used, indicating a substantial reduction in image motion. Quantitatively, when we examine the power spectrum on the X axis, the corrected spectrum (shown in black) begins to converge with the uncorrected spectrum (in blue) at approximately 80 Hz, which is referred to as the cut-off frequency. Beyond this point, the uncorrected power spectrum exhibits notably lower power compared to the corrected one. A similar trend is observed on the Y axis, with both spectra merging around the same approximate frequency. Nevertheless, beyond this frequency, the corrected spectrum shows only marginal improvement over the uncorrected spectrum. It was also noted that the image movement when giving feedback to second mirror M2 is not smooth. When the second mirror moves, it induces pronounced vibrations, causing oscillations of the image on the image plane. A notable observation was the clear correlation between the moment feedback was provided to mirror M2 and the occurrence of large image shifts (not shown). Thus, there is a possibility of further improvement of the image stabilization system after the vibrations of the mirror M2 are addressed.

In conclusion, the image stabilization system, comprising the tip–tilt system and autoguider system, performs with a cut-off frequency of 80 Hz. There is a potential for improvement by addressing the vibrations of mirror M2 of KTT.

4. SEEING-INDUCED CROSSTALK IN THE POLARIZATION MEASUREMENTS

The Earth's dynamic atmosphere causes crosstalk in the polarization measurements. Variations over time in the Earth's atmosphere result in wavefront distortions, subsequently causing spatial blurring of images and polarization. To mitigate the blurring of Stokes parameters, image stabilization methods like tip–tilt and AO systems are used. However, these techniques cannot eliminate the intermixing of Stokes parameters, known as seeing-induced crosstalk, which results from the slow modulation process compared to the rapid fluctuations induced by atmospheric conditions, occurring at frequencies around 500 Hz. If the modulation frequency is on the order of 1 kHz, the seeing-induced crosstalk is not of much concern; however, it is challenging to achieve [1,2,11]. Consequently, the Stokes parameter I_A measured at the telescope's entrance aperture following the propagation of light through the atmosphere is

$$I_A = I_l + \langle \delta I_l \rangle + \delta I_l, \tag{1}$$

where $\langle \delta I_l \rangle$ represents the spatial smearing (time averaged) of true Stokes parameter I_l due to atmospheric conditions, which we neglect assuming the tip–tilt system is operational and δI_l are spurious polarization features induced due to the slow modulation frequency.

Let O be the modulation matrix of the combined system consisting of telescope optics and the polarimeter, then the recorded modulated intensities $I_{\mathrm{meas},k}$ for the kth modulation state are given by

$$I_{\mathrm{meas},k} = \sum_{l=1}^{4} O_{kl}(I_l + \delta I_{lk}), \tag{2}$$

where δI_{lk} is the spurious polarization feature δI_l introduced to the kth modulation state. The Stokes vector (I_{infer}) is extracted from the measured intensities by multiplying the demodulation matrix (D) with modulated intensities (I_{meas}), expressed as

$$I_{\mathrm{infer},1} = I_1 + \sum_{k=1}^{4}\sum_{m=1}^{4} D_{1k} O^T_{km} \delta I_{mk},$$

$$I_{\mathrm{infer},l} = I_l + \sum_{k=1}^{4}\sum_{m=1}^{4} D_{lk} O^T_{km} \delta I_{mk} \quad \text{for } l = 2,\ 3,\ \text{and } 4, \tag{3}$$

where D can be calculated from the modulation matrix (O) by

$$D = (O^T O)^{-1} O^T. \tag{4}$$

The dual-beam polarimetry technique is commonly employed to reduce the impact of seeing-induced crosstalk (specifically $Q, U, V \rightarrow I$ and $I \rightarrow Q, U, V$). In the polarimeter setup, a polarizing beam displacer is employed as the analyzer instead of a single linear polarizer. This allows for the simultaneous recording of intensities from two orthogonally polarized beams. The intensity in each beam is modulated with same sign while the remaining Stokes parameters ($Q/U/V$) are modulated with opposite signs. This is due to the elements in the first column of the modulation matrix being equal to "1," and the remaining elements of the modulation matrix having equal magnitude but opposite signs in the two orthogonally polarized beams. By averaging the Stokes parameters obtained from both beams, crosstalk $Q, U, V \rightarrow I$ as well as $I \rightarrow Q, U, V$ is effectively neutralized. The $I \rightarrow Q, U, V$ crosstalk specifically is determined by halving the difference in Stokes parameters measured from the two oppositely polarized beams. For more details, please refer to Chapter 5, p. 68, of [11].

5. MEASUREMENTS OF SEEING-INDUCED CROSSTALK IN THE POLARIZATION MEASUREMENTS

The polarimeter at KTT is a dual-beam system [7]. As explained in the previous section, the Stokes parameters are typically determined independently from each of the two orthogonally polarized beams and then averaged to reduce the spurious signals caused by atmospheric turbulence. In order to compare the seeing-induced crosstalk before and after implementing the tip–tilt system, we analyze the residuals of the Stokes parameters in the wing positions of the H α and Ca II 8662 Å lines. These residuals are calculated by halving the difference between the Stokes parameters independently derived from each of the two beams. The residuals of the Stokes parameters represent the seeing-induced crosstalk ($I \rightarrow Q, U, V$). Figure 3 shows the wavelength regions selected (shown by black vertical lines) for calculating the residuals. The wavelength region selected for Ca II 8662 Å line is comparatively inside the line than that of H α line because there were considerable fringes present in the raw data that were removed during post-processing. This context image is made from the aligned, fringe-removed merged beam data. The mean and root mean square (rms) values of the rms values of the crosstalk of different terms in the H α and Ca II 8662 Å lines are compared in Table 1. The histogram of the rms values of the Stokes Q/I, U/I, and V/I residuals of the H α and Ca II 8662 Å lines are shown in Figs. 4 and 5, respectively.

The H α residual spectrum exhibits residual levels as high as 0.06 (6%) for Stokes Q/I, 0.07 (7%) for Stokes U/I, and 0.08 (8%) for Stokes V/I without the tip–tilt system. However, with the tip–tilt system, the maximum residual value significantly reduces to 0.014 (1.4%) for Stokes Q/I and U/I and 0.03 (3%) for Stokes V/I, and the spread of the distribution narrows, with most pixels having residuals around 0.003 (0.3%) for Stokes Q/I and U/I and 0.005 (0.5%) for Stokes V/I. The rms value of residual also decreases by factors of 3.6, 2.7, and 2.5 for Stokes Q/I, U/I, and V/I, respectively. Similarly, in the Ca II 8662 Å spectrum, the value of the residuals can reach up to 0.06 (6%) for Stokes Q/I, 0.05 (5%) for Stokes U/I, and 0.04 (4%) for Stokes V/I without the tip–tilt system but decreases to 0.015 (1.5%) for Stokes Q/I, 0.013 (1.3%) for Stokes U/I, and 0.02 (2%) for Stokes V/I when the tip–tilt system is employed. The rms value of the residual decreases by factors of 2.8, 2.2, and 1.8 for Stokes Q/I, U/I, and V/I, respectively. The distribution in the Ca II 8662 Å distribution also narrows, with most pixels having noise around 0.005 (0.5%) for all Stokes parameters. Using image motion power spectra, Judge *et al*. [2] reported the $I \rightarrow Q, U, V$ crosstalk of about ~ 0.006 for rotating retarders based polarimeters after tip–tilt correction, which is comparable to the rms crosstalk observed in the tip–tilt corrected H α and Ca II 8662 Å spectrum.

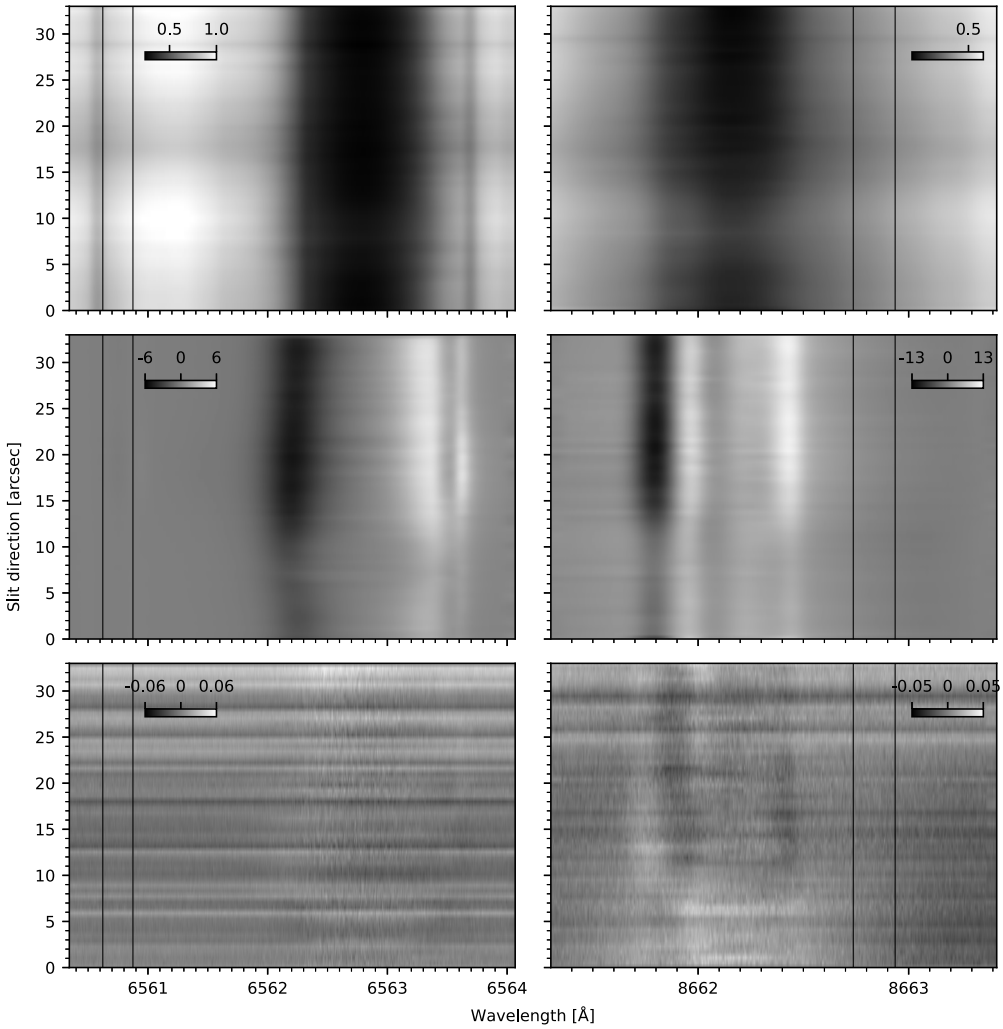

Fig. 3. Spectral image showing the wavelength regions selected (black vertical lines) for calculating residuals. The left column shows data for H α line while right column shows data for Ca II 8662 Å line. The top row shows spectral image of Stokes I, while middle row shows spectral image of Stokes V/I [%]. The bottom row shows the residuals for the H α and Ca II 8662 Å lines, respectively.

Table 1. Comparison of Mean and rms Crosstalk Values of Different Terms of H α and Ca II 8662 Å Lines

Line	Term	Uncorrected Mean	Corrected Mean	Uncorrected rms	Corrected rms
H α	$I \rightarrow Q$	0.012	0.004	0.018	0.005
H α	$I \rightarrow U$	0.013	0.005	0.019	0.007
H α	$I \rightarrow V$	0.016	0.007	0.023	0.009
Ca II 8662 Å	$I \rightarrow Q$	0.012	0.005	0.017	0.006
Ca II 8662 Å	$I \rightarrow U$	0.007	0.004	0.011	0.005
Ca II 8662 Å	$I \rightarrow V$	0.008	0.005	0.011	0.006

We note here that the crosstalk estimated in the data does not exist in the reduced science ready data; it is only brought out to show the effect of the tip–tilt system in reducing the crosstalk. Despite the widespread use of tip–tilt systems in solar telescopes [5], no such direct measurements of seeing-induced crosstalk have been reported in the literature. A manuscript describing the measurements of seeing-induced crosstalk with and without the tip–tilt system carried out at the German Vacuum Tower Telescope (VTT [12]) using Tenerife Infrared Polarimeter (TIP-II [13]) instrument is in preparation by Nagaraju *et al.* (private communication). Our conclusion from this analysis is that the tip–tilt system implemented at KTT noticeably decreases the rms crosstalk by a minimum factor of 2.

6. CONCLUSION

We have presented measurements of the crosstalk in Stokes parameters induced by atmospheric seeing with and without the tip–tilt system in use. This was done to show the effect of the tip–tilt system in reducing the seeing-induced crosstalk. In

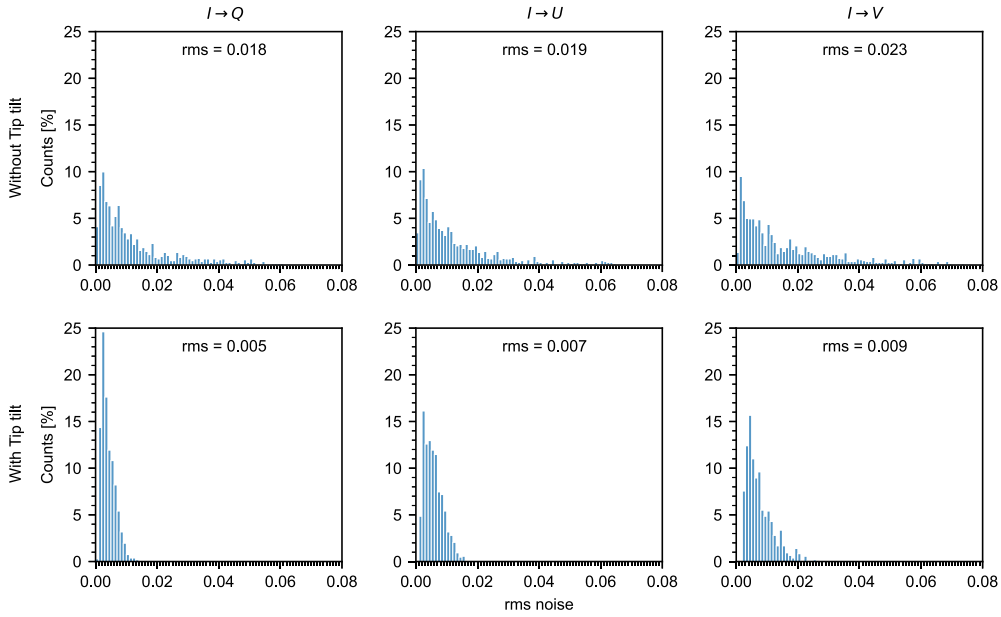

Fig. 4. Analysis of seeing-induced crosstalk in polarimetric measurements for the H α line is conducted with and without the implementation of a tip–tilt system. In the top row, we show the histogram of the root mean square (rms) of the residuals without the tip–tilt system for Stokes Q/I, U/I and V/I, column-wise, respectively. The bottom row shows the histograms when the tip–tilt system was operational. The rms residual was determined by calculating residuals of the Stokes parameters in the wing of the H α line. The Stokes parameters were independently determined from each beam and then subtracted and halved to give the residual. The results reveal a significant reduction in the rms residual, with Stokes Q/I showing a decrease by a factor of 3.6, Stokes U/I showing a decrease by a factor of 2.7, and Stokes V/I showing a decrease by a factor of 2.5.

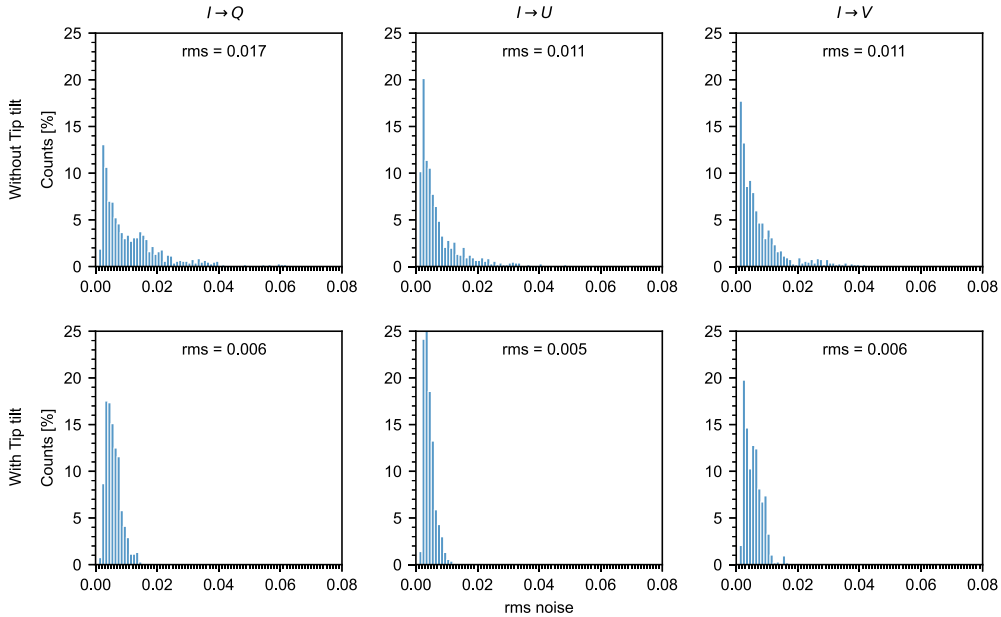

Fig. 5. Similar to Fig. 4, but for the Ca II 8662 Å line. The results reveal a significant reduction in rms residual, with Stokes Q/I showing a decrease by a factor of 2.8, Stokes U/I showing a decrease by a factor of 2.2, and Stokes V/I showing a decrease by a factor of 1.8.

that context, we have integrated and installed a tip–tilt system with an autoguider system to arrest the residual image motion. The tip–tilt system is shown to have a cut-off frequency of 80 Hz, keeping image shifts within ±0.11 95% of the time. Two new cameras, a Kinetix from Teledyne and Orca Quest from Hammamatsu, are installed on the spectroscopic focal plane to record the H α and Ca II 8662 Å spectrum simultaneously. With the help of the image stabilization system, the seeing-induced crosstalk measured in the Stokes parameters of the H α and Ca II 8662 Å spectrum is shown to be reduced by at least a factor of 2.

Funding. Indian Institute of Astrophysics.

Acknowledgment. HM acknowledges R. Sridharan for various discussions on the operation of the tip–tilt system and Jayant Joshi for various

discussions on adaptive optics and high-resolution observational techniques, which were immensely helpful while recording these observations. HM acknowledges Mr. Udayakumar, Mr. Devendran, Mr. Ramesh, and the KoSO mechanical and telescope support team for their help and support in promptly operating the telescope. Harsh Mathur handled most of the optical setup, conducted observations, analyzed the data, and wrote the manuscript. K. Sagaynathan and the mechanical team created mounts for cameras and optical components. Hemanth Pruthvi assisted in optimizing the tip–tilt and polarimeter setup. K. Nagaraju is the project's principal investigator (PI), and all authors contributed to the manuscript through discussions.

Disclosures. The authors declare no conflicts of interest.

Data availability. Data underlying the results presented in this paper are not publicly available at this time but may be obtained from the authors upon reasonable request.

REFERENCES

1. B. W. Lites, "Rotating waveplates as polarization modulators for Stokes polarimetry of the sun: evaluation of seeing-induced crosstalk errors," Appl. Opt. **26**, 3838–3845 (1987).
2. P. G. Judge, D. F. Elmore, B. W. Lites, *et al.*, "Evaluation of seeing-induced cross talk in tip-tilt-corrected solar polarimetry," Appl. Opt. **43**, 3817–3828 (2004).
3. K. Nagaraju and A. Feller, "Precision in ground-based solar polarimetry: simulating the role of adaptive optics," Appl. Opt. **51**, 7953–7961 (2012).
4. J. C. del Toro Iniesta and M. Collados, "Optimum modulation and demodulation matrices for solar polarimetry," Appl. Opt. **39**, 1637–1642 (2000).
5. T. R. Rimmele and J. Marino, "Solar adaptive optics," Living Rev. Sol. Phys. **8**, 2 (2011).
6. K. Nagaraju, A. Feller, S. Ihle, *et al.*, "Atmospheric turbulence and high-precision ground-based solar polarimetry," Proc. SPIE **8148**, 81480S (2011).
7. H. Pruthvi, N. Krishnappa, R. Belur, *et al.*, "Solar spectropolarimetry of Ca II 8542 Å line: polarimeter development, calibration, and preliminary observations," J. Astron. Telesc. Instrum. Syst. **4**, 1 (2018).
8. M. K. V. Bappu, "Solar physics at Kodaikanal," SoPh **1**, 151–156 (1967).
9. H. Mathur, K. C. Thulasidharen, H. Pruthvi, *et al.*, "An image auto guider system for Kodaikanal Tower Tunnel Telescope," J. Astron. Instrum. **11**, 2350003 (2022).
10. H. Pruthvi, "Design and development of chromospheric vector magnetograph for sunspot studies," Ph.D. thesis (IIA Institutional Repository, 2019).
11. J. C. del Toro Iniesta, *Introduction to Spectropolarimetry* (Cambridge University Press, 2007).
12. O. von der Lühe, "High-resolution observations with the German Vacuum Tower Telescope on Tenerife," New Astron. Rev. **42**, 493–497 (1998).
13. M. Collados, A. Lagg, J. J. Díaz, *et al.*, "Tenerife infrared polarimeter II," in *The Physics of Chromospheric Plasmas*, P. Heinzel, I. Dorotovič, and R. J. Rutten, eds., Vol. **368** of Astronomical Society of the Pacific Conference Series (2007), p. 611.